Procedia Manufacturing

Volume 5, 2016, Pages 282–294

44th Proceedings of the North American Manufacturing Research Institution of SME http://www.sme.org/namrc

Influence of Laser Heat Treatment on Machinability of Ti6Al4V Alloy

Sagar Telrandhe[1*], Ashish K Saxena[2], Pavan Sutar[3] Sushil Mishra[1$]

[1]*Department of Mechanical engineering,*
Indian Institute of Technology Bombay, Mumbai, India.
[2]*Department of Metallurgical Engineering & Materials Science,*
Indian Institute of Technology Bombay, Mumbai, India
[3]*Bharat Forge Limited, Pune, India.*
[*]*sagar.telrandhe@iitb.ac.in*, [$]*sushil.mishra@iitb.ac.in*

Abstract

Titanium alloys are most extensively used in biomedical application, which need high degree of dimensional accuracy and good machinability to reduce manufacturing cost. Both of these necessities can be addressed by surface and sub-surface modification without altering the mechanical properties in core of the material. The laser treatment is one of best tool to obtain controlled surface modification. In present paper the laser treatment directionality effect on subsurface modification is studied and correlated with machinability of Ti6Al4V. The reduction in cutting force variation is observed for unidirectional laser treated sample, which contribute to enhance the machinability of the alloy.

Keywords: Subsurface modification, laser treatment, Directionality effect, Force variation

1 Introduction

Titanium alloys are considered vital role especially in aerospace and biomechanical applications (Leyens & Peters 2006). In both of these fields, machining process plays an important role in order to get the high degree of dimensional accuracy (Ezugwu & Wang 1997) in component manufacturing. Among all titanium alloys, Ti6Al4V is most extensively used (Matthew J. Donachie 2000). However, its high strength, low modulus and lower thermal conductivity makes it difficult to machine (Khanna et al. 2012; MacHai & Biermann 2011). The lower thermal conductivity, in particular, is the sole reason for segmented chip formation. This segmented chips leads to large force variation on cutting tool. This force variation cause due to segmented chip which leads to deterioration of tool life (Kouadri et al. 2013). Though the average magnitude of cutting forces during titanium machining is

 Selection and peer-review under responsibility of the Scientific Programme Committee of NAMRI/SME

doi:10.1016/j.promfg.2016.08.025

lower as compared to high strength steel, the vibration caused by force variation is higher during machining of titanium alloys.

Several studies were focused to reduce the formation of shear bands, which causes chip segmentation (Patil et al. 2014; Zhan et al. 2014; Dargusch et al. 2008). Use of coolants and induction of cyclic vibrational motion on cutting tool proven to be an effective methods in reducing the vibration and magnitude of cutting forces (Ezugwu et al. 2003; Edkinsa et al. 2014). The cryogenic environment machining was also introduces in order to reduce the heating effect near the tool tip (Courbon et al. 2013; El-Tayeb et al. 2009). Another concept of hybrid machining was introduced, in which the material was preheated below recrystallization temperature before machining; this causes reduction in the temperature gradient (Joshi et al. 2014; Arrazola et al. 2013; Lee et al. 2015), moreover, the basal slip system $\{0\ 0\ 0\ 1\}\langle 1\ 1\ \bar{2}\ 0\rangle$ gets activated providing an ease in plastic deformation during machining (Babu & Lindgren 2013). The preheating can be done by means of following methods:

- Gas-flame heating
- Resistance heating
- Light Amplification by Stimulated Emission of Radiation heating (Laser heating)

In gas flame and resistance heating, a larger surface area near tool tip get influenced by preheating leads to rapid flank wear due to high temperature at chip-tool interface (Upadhyay et al. 2012). However, the laser heating provides a controlled surroundings in terms of temperature ranges and positions. That is why the concept of Laser assisted machining has been introduced (Alhammad et al. 2008; Ayed et al. 2014). In laser assisted machining (LAM), the preheating is done on the localized region of workpiece ahead of cutting tool edge. The intensity of laser is adjusted in such a way that the cutting tool doesn't come under the influence of temperature variations. Further, only a localized zone of workpiece comes under the laser scanner which does not affect the microstructure of rest of the material. However, the LAM has certain limitations such as sophisticated working environment to couple with machining, intensities can be optimized in minimum range so that the temperature rise should not damage the cutting tool. Although the LAM provides well controlled localized heating prior to machining, the temperature increment is restricted beyond 600^{o}C (approximately) (Ayed et al. 2014). This restriction is imposed to protect the cutting edge of tool from blunting.

The present work is an attempt to make use of laser power with low scanning speed in subsurface modification. The modification of surface and subsurface microstructure has been done by increasing the temperature through laser heat source beyond recrystallization temperature of material. This leads to substantial microstructural changes in material which cannot be attain through LAM. The laser heating at localized region effects in rapid quenching as since, the whole rest of material acts as a sink. Prior to machining, the microstructure of sub-surface has been modified in order to study its effect on machining behavior of Ti6Al4V.This study has been broadly classified in three sections:

- Effect of laser treatment on annealed samples.
- Changes observed in microstructure because of laser treatment.
- Effect of laser treatment on machining.

2 Experimental details

Laser treatment: The laser treatment was performed in Ytterbium fiber laser system of 1.08 μm wavelength for Ti-6Al-4V surface and subsurface modification. Figure 1 shows the schematic of surface and subsurface modification setup via laser source (shown in red color). The laser spot diameter was 2.35 mm. The specification for laser system is given in table 1. To ensure continuity in

laser treatment on each sample, an overlap of 1 mm is given in helix pattern with constant feed of 1 mm/rev. While performing laser treatment, a thermal camera was used to get fairly accurate temperature range of heating via temperature observation. The operating parameters were optimized such that Ti6Al4V alloy should not reach beyond the β-transus zone.

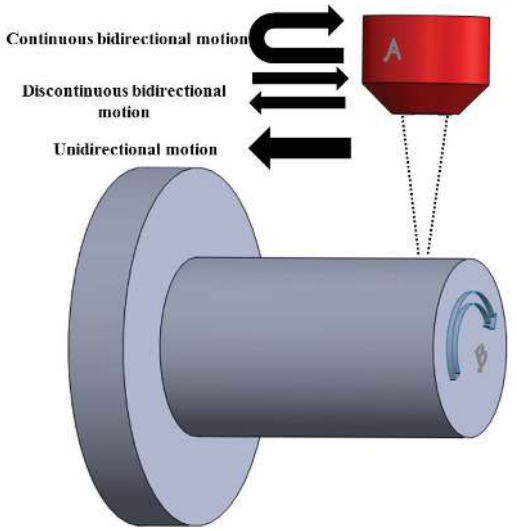

Figure 1: Schematic of laser treatment, A) Source, B) sample fixed inside rotary chuck

Table 1: Laser treatment specification

Laser parameter	Specification
Wavelength	1080 nm
Maximum Power ,P max	2100 W
Operation Mode	Continuous and Pulse

Microstructure analysis: Commercially available Ti6Al4V alloy has been polished using automatic polishing machine. At first, the sample has been hot mounted using bakelite powder (thermosetting plastic polymer). The mounting is used to prevent the subsurface from blunting during polishing process. This polishing starts with rotating the disc MD-Piano 120 with water poured on it. At second stage, MD-Largo disc is used with 9 µm diamond suspension. At third stage, a chemical-mechanical polishing method is followed with the mixture of colloidal silica 0.5 µm (OP-S) and 50 % of water poured on MD-Chem disc to get mirror polish. For the analysis through optical microscope, Kroll's reagent was used to perform chemical itching. In last stage, electro polishing was carried out through A2 electrolyte (STRUERS) to see the surface during EBSD (Electron Back-scattered Diffraction) analysis. The EBSD scans are helpful in order to determine the grain size, its texture and changes in it due to laser treatment. The EBSD scans were taken with 0.2 µm step size. Scans were carried out with help of FEI Quanta scanning electron microscope which is coupled with TSL OIM orientation and imaging microscopy software. Further only those measured points were considered for analysis which are above 0.1 confidence index (CI) to get accuracy in quantification.

Machining process: Machining process was carried out on Ti64 rod (ϕ=10 mm). CNC lathe has been used to perform turning operation. The Ti64 alloy rod has undergone metal cutting process at

cutting velocity of 1.83 m/s. Feed and depth of cut were fixed as 0.3 mm/rev and 0.625 mm respectively for all procedures. The rake angle and relief angle were taken as 0°and 3°respectively. For each metal removal process, a new carbide insert were used to get dimensional accuracy. The machining operation was performed in dry conditions. The cutting forces were measured by online method using Kistler dynamometer (Model 9257). The output from the dynamometer is amplified through a charge meter (Kistler Corporation Model 5015A). It was linked together by a highly insulated resistance cable connected to a charge amplifier, which in turn is connected to analog to digital converter and the data acquisition hardware/software installed in the computer.

3 Results and discussion

The laser treatment was performed with the optimal combination of laser power and scanning speed. With these two input parameters, the energy density calculated by using following equation:

$$E = \frac{P}{d * v}$$

Where, E is energy density of continuous laser beam (J/mm^2), P is laser power (W), d is spot diameter (mm) and v is scanning velocity as $v = \pi dN$, where N is rotational speed of workpiece.

While performing trials, it was observed that the material reaches to red hot condition, when the energy level is 16 J/mm^2 and begin to melt at 20 J/mm^2. Thus to avoid both of these effects, the laser power was restricted to 300 W for present set of experiments. To analyze the changes occurred in the material which could later affect the machining process, the current section is divided in two parts:

- Microstructure analysis of laser treated samples
- Effect of laser-treatment on machining

As-received Ti6Al4V rods were pre-annealed at 835°C for 4 hours followed by furnace cooling to attain uniform and strain free grain structure. Laser treatment was performed by moving the laser source in continuous and discontinuous, back and forth motion for 200 mm length. For discontinuous laser treatment, the sample was cooled until it reaches to room temperature before starting the second pass. In third case, this laser source was moved only in one direction to the length of 200 mm.

The laser penetration depth was studied by optical microscopy on cross-section of cylindrical laser treated samples. The micrograph in Figure 2a shows the non-uniformity in microstructure of laser affected zone. To closely analyze the non-uniformity in microstructure, figure 2a is divided into six parts which shows transition in microstructure from laser treated edge towards center. Figure 2b shows microstructure near the edge of laser treated sample, whereas Figure 2c shows the region of 100 µm to 250 µm from edge. Likewise, Figure 2(d-g) shows the successive transformation in microstructure at equal intervals of 150 µm. Needle-like flakes structure is observed close to the edge as shown in figure 2 (b & c). The intensity of uniform flakes decreases in figure 2d. And transition zone shows presence of both flakes and equiaxed grains (figure 2f). The presence of flakes gets nullified as move towards the center of the sample (Figure 2b-f), since the laser penetration is limited to a particular depth. And finally the completely equiaxed grain structure is obtained at about a distance of 700 µm from the edge of laser treated sample. The depth of laser modified layer through laser treatment is measured by the optical micrographs. As per the change in the microstructure complete processing zone can be divided two regions; near edge zone which has high density flaks like structure and transition zone has mixed microstructure with flaks as well as the equiaxed grains.

The depth of cut for machining is decided such that the effect of laser processing during machining can be captured through the experiments.

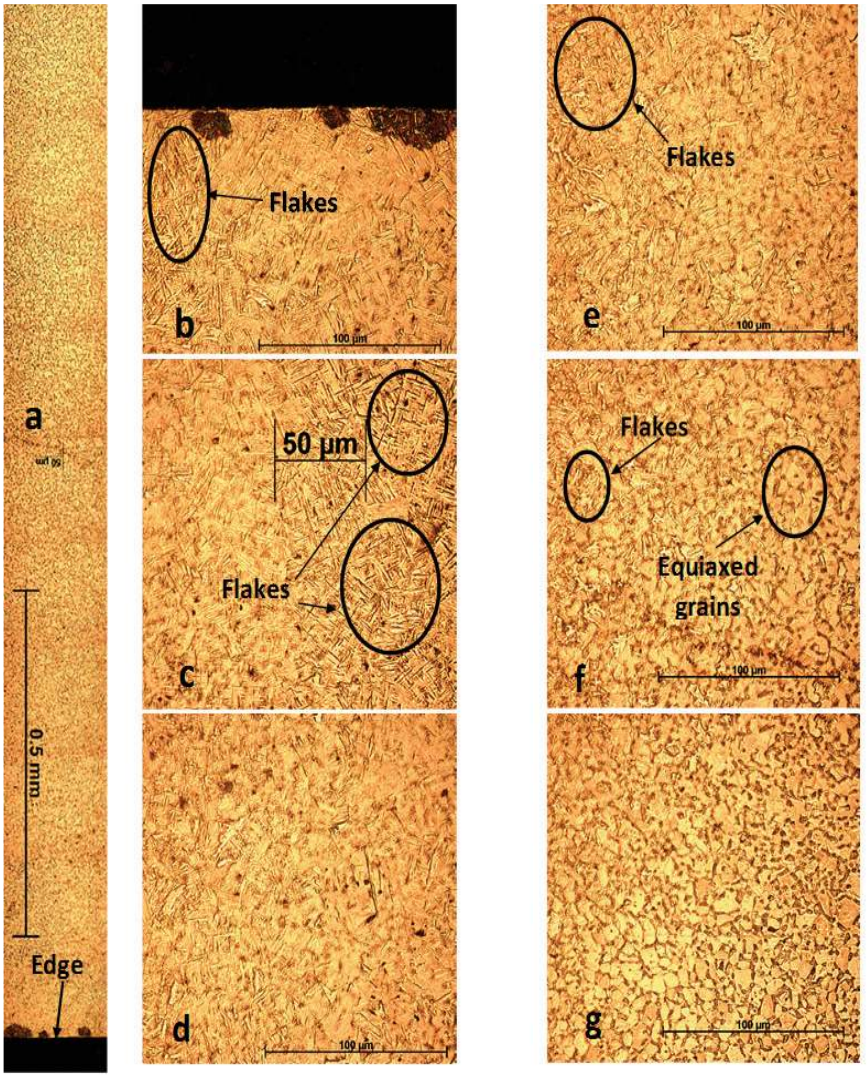

Figure 2: (a) Optical image of laser treated sample (with unidirectional scanning) from edge to center, (b) enlarged optical image near edge with predominant needle-like structure with flakes, (c-f) transition of microstructure from flakes to equiaxed grains and (g) complete equiaxed structure at 700 µm from edge.

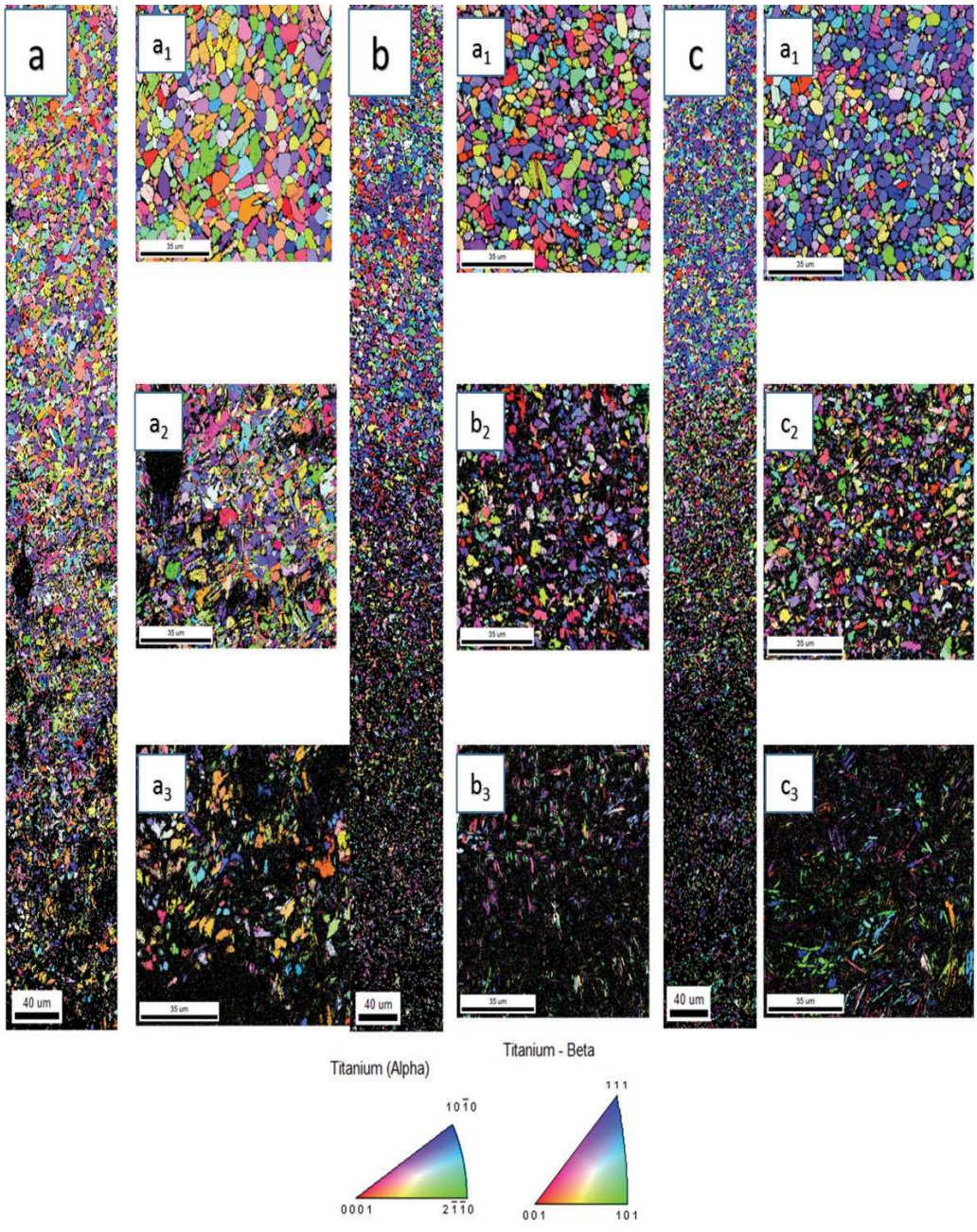

Figure 3: (a) Inverse pole figure (IPF) map for sample undergone bidirectional continuous laser treatment, (b) IPF map for bidirectional discontinuous laser treated sample and (c) IPF map for unidirectional laser treated sample.

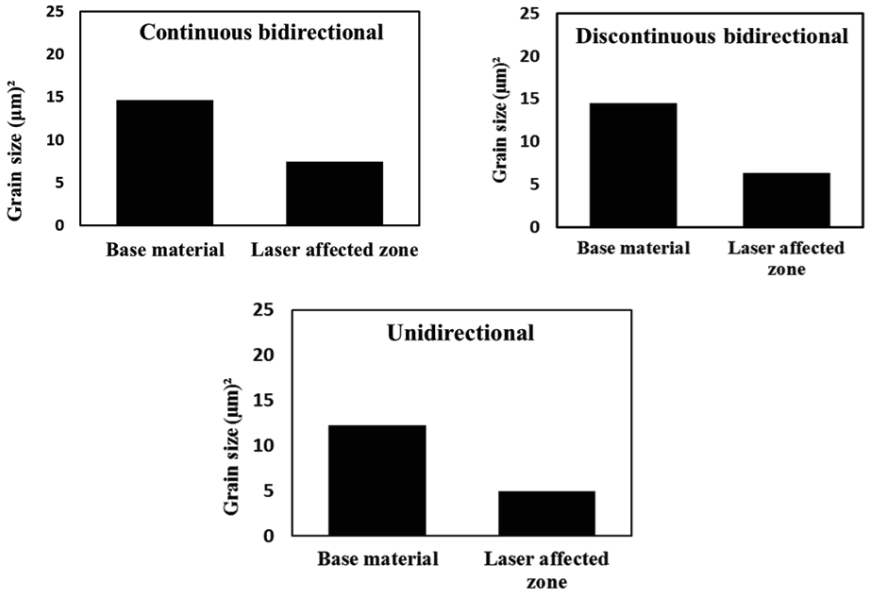

Figure 4: Grain size variation between laser affected zone and base metal considering directionality effect of scanning.

Through optical analysis, it has been observed that the density of flakes is larger near the edge of sample from where laser beam was passed. For every sample in present set of experiment, this larger flakes density was seen approximately upto 140 μm. This density then observed to be varied in transition region for unidirectional and bidirectional laser scanning. The reason of this variation cannot be exactly quantified through optical micrographs as it does not give details about orientation distribution and occurrence of phase change during laser treatment. Thus EBSD scans were taken in the same processed area and this can capture the strain localization due to rapid quenching while processing.

The EBSD scans was taken for all the three laser treatment cases as mentioned earlier, is shown in figure 3. Both α (HCP) and β (BCC) phases of titanium alloy were included in database while taking EBSD scan. In all scans, it is observed that there is no dominance of particular orientation because of laser treatment. A series on non-indexing points in EBSD is observed near heat affected area of processed sample. In EBSD scan, the non-indexed points occur because of three particular reasons: 1) dislocation pileup, 2) strain localization and 3) phase change. As there is no plastic deformation throughout the laser scanning process, so dislocation movement and pile-up cannot contribute to this non-indexing. However, due to combine effect of lasering and rapid quenching, there is a possibility of both strain localization as well as phase change in the material (Hu & Botten 2002; Popov et al. 2014). The α-titanium flakes has been observed predominantly in case of unidirectional scanning (figure $3c_3$). The traces of flakes is also visible in discontinuous laser scanning (figure $3b_3$), whereas, for continuous and bidirectional laser scanning samples (figure $3a_3$), very few flakes has been formed. The reason behind this is the heat accumulation due to continuous energy supply for longer duration of time, which allows the grains to attain a granular shape.

The middle part of all EBSD scans shows the transition zone, which is similar as observed in optical micrograph. In this zone, trace of equiaxed grain structure has been found with less number of non-indexing points because of lowered laser penetration. A uniform distribution of grains has been

observed as the depth of laser penetration nullified towards center of sample. The grain size in the transition zone is reduced due to laser treatment. While taking size of grains in consideration, grain in transition zone was compared to the grains shown in the region a_1, b_1 and c_1 of figure 3. The comparison of grain size is given in figure 4. The reduction in grain size is about 60 % for all laser treatment. This reduction has well attributed to increase in hardness of laser affected zone as shown in figure 5. Hardness measurements were carried out at two places in laser affected zone which includes the zone with flakes and as well as transition zone. Uniform increment in hardness has been accounted for all three experimental conditions. The hardness variation at localized level is an output of temperature gradient between source and sink (the sink is considered as rest of the material which is not under laser spot during laser scanning). While performing laser scanning, the temperature was varying from 950^0C to 1100^0C along the axis for unidirectional laser scan measured through infra-red camera. For bidirectional continuous laser scanning (continuous double pass), temperature variation for first pass was same as for unidirectional laser scanning. During second pass, the temperature was varying from 1180^0C to 1320^0C along the axis. Whereas, for bidirectional dis-continuous laser scanning, material was allowed to cool after first pass. During second pass, the temperature was varying from 1120^0C to 1350^0C.

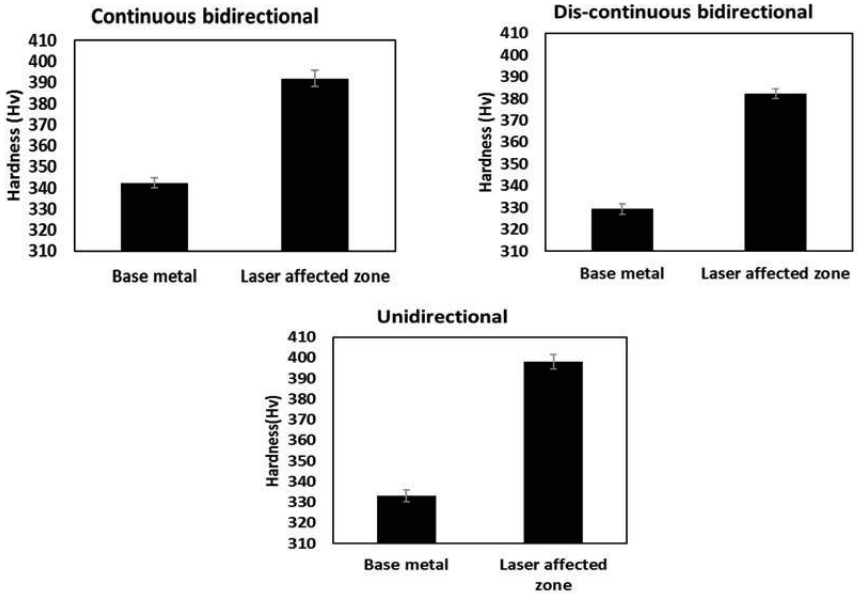

Figure 5: Micro hardness variation between laser affected zone and base metal considering directionality effect of scanning.

In the second part of analysis, all the laser treated samples were machined. In this study, the variation in cutting forces is observed, as it is the primary reason for tool damage during machining of titanium alloys (Upadhyay et al. 2013). The uncut chip thickness is kept well within the range of laser affected zone (since, laser treatment has been done uniformly around the circumference). After analyzing figure 6, it is found that the average feed force in case of laser treated samples is more as compared to non-treated sample. The increase in feed forces is due to rise in hardness, which is because of grain size reduction or/and possible development of new phase as discussed earlier. However, there is no significant change has been observed in feed force variation. Moreover, after machining laser treated samples, a significant amount of reduction in cutting forces variation has been observed in case of sample undergone unidirectional laser treatment treated sample, as it has

predominant flakes (needle like) structure. This structure shows the material has undergone martensitic transformation as discussed earlier (Vrancken et al. 2012). This transformation arrest the plastic deformation of shear bands. The cutting force variation through force measurements does not provide a clear indication of force variation in present analysis, hence a detail study of chip segmentation can present a better way to analyze the force variation.

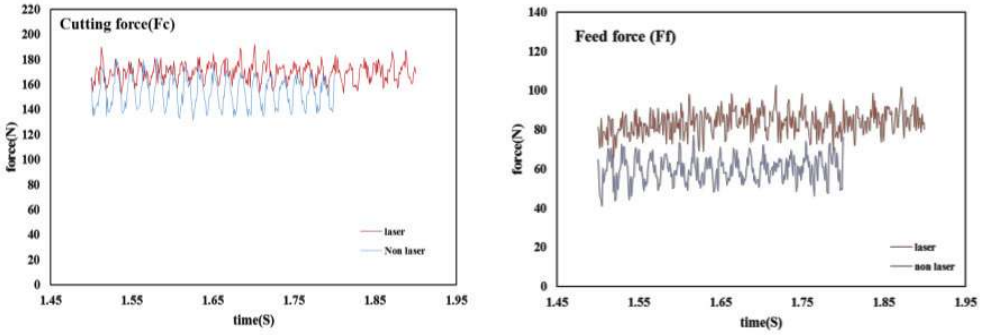

(a) Continuous bidirectional

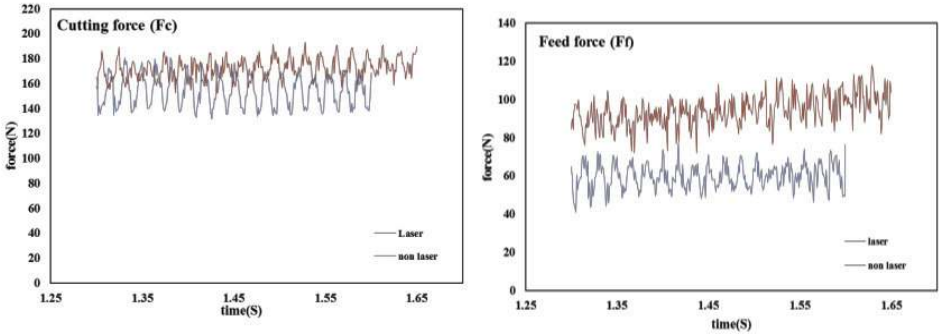

(b) Discontinuous bidirectional

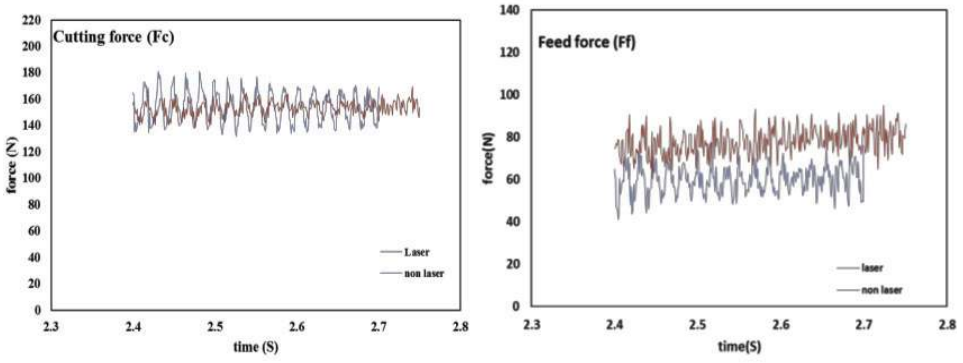

(c) Unidirectional

Figure 6: Comparison of variation in feed force and cutting force between laser treated (red) and non-heat treated (blue) sample considering directionality effect of scanning.

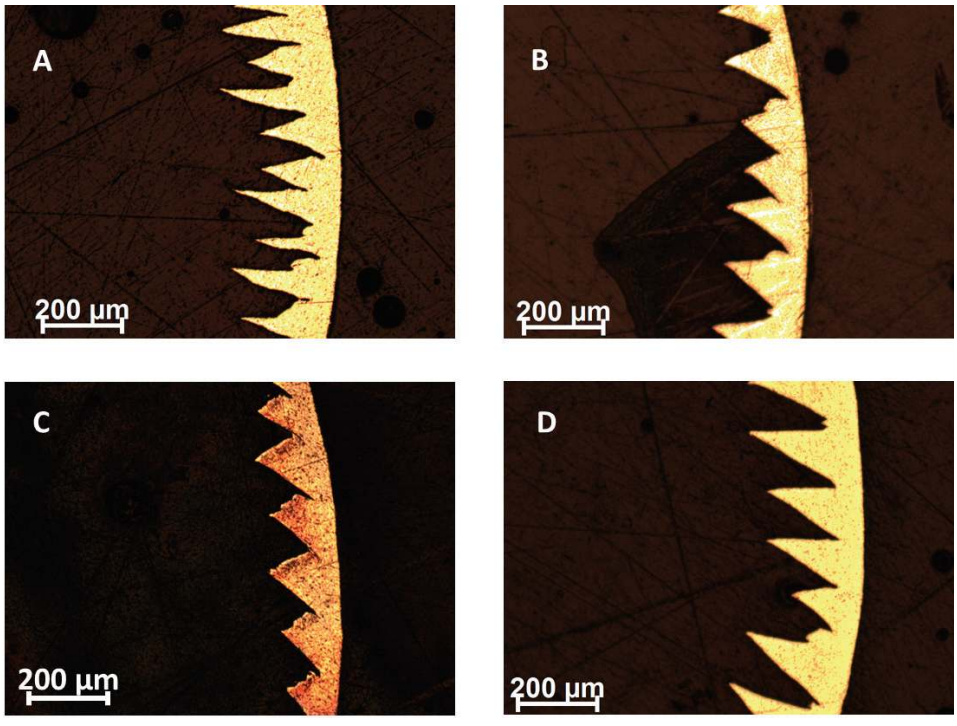

Figure 7: Comparison of variation in chip segmentation between non-laser treated (A) and (B) continuous bidirectional (C) discontinuous bidirectional and (D) unidirectional laser treated sample.

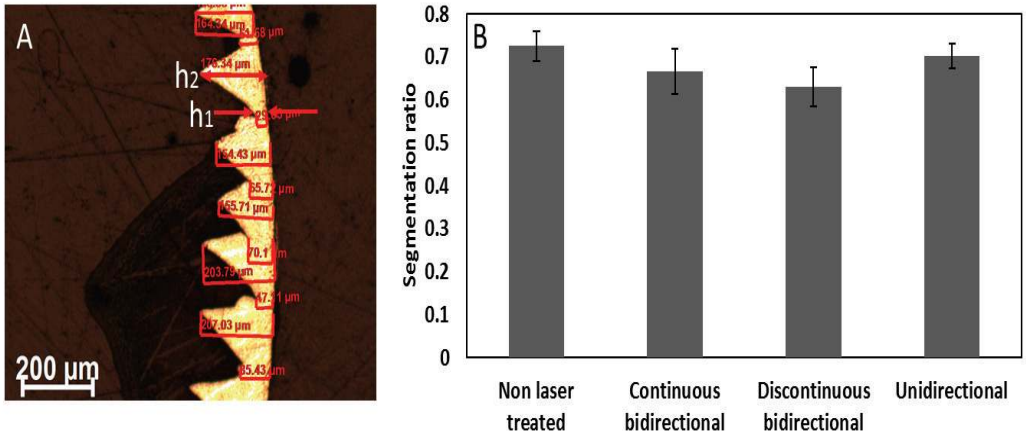

Figure 8: A) Measurement of segmentation ratio through micrograph of machined Ti6Al4V chips B) Segmentation ratio comparison between laser treated and non-treated machined samples.

For this purpose, the chips of all the samples (laser treated and non-laser treated undergone machining has been collected and its morphology has been examined under optical microscope. Figure 7 shows chip segmentation comparison between non-laser treated (figure 7a) and laser treated (figure 7 b, c & d) machined sample. Further, figure 8 shows the comparison of segmentation ratio. The segmentation ratio is the ratio of $\frac{h_2-h_1}{h_1}$ (as given if figure 8). This ratio is found to be lesser in all laser treated samples. The least segmentation has been found in discontinuous bidirectional sample.

4 Conclusion

Considering combine effect of laser treatment and its directionality on surface and subsurface modification of Ti6Al4V alloy, following conclusions were made:

1 The directionality of laser scanning significantly affects the flake structure density in processed microstructure of Ti6Al4V. Unidirectional, continuous bidirectional and discontinuous bidirectional laser scanning causes the change in flakes density in the laser processed zone.
2 High flakes density developed during unidirectional laser scanning reduces the variation in cutting forces. This reduction in cutting force variation improves the overall machinability of Ti6Al4V.
3 The laser scanning increase in the hardness in processed zone, which in turn causes increase in average feed force.

Acknowledgement

The authors gratefully acknowledge the funding support provided by National Center for Aerospace Innovation and Research (NCAIR), IIT Bombay for the project. Authors also acknowledge the Lasering and Machining facility at Machine Tool Lab, Mechanical dep., IIT bombay and EBSD facility OIM lab, MEMS dept, IIT Bombay.

References

Alhammad, M., Esmaeili, S. & Toyserkani, E., 2008. Surface modification of Ti-6Al-4V alloy using laser-assisted deposition of a Ti-Si compound. *Surface and Coatings Technology*, 203(1-2), pp.1–8.

Arrazola, P.J. et al., 2013. Recent advances in modelling of metal machining processes. *CIRP Annals - Manufacturing Technology*, 62(2), pp.695–718.

Ayed, Y. et al., 2014. Experimental and numerical study of laser-assisted machining of Ti6Al4V titanium alloy. *Finite Elements in Analysis and Design*, 92, pp.72–79. Available at: http://linkinghub.elsevier.com/retrieve/pii/S0168874X14001619.

Babu, B. & Lindgren, L.-E., 2013. Dislocation density based model for plastic deformation and globularization of Ti-6Al-4V. *International Journal of Plasticity*, 50, pp.94–108. Available at:

http://www.sciencedirect.com/science/article/pii/S0749641913000910.

Courbon, C. et al., 2013. Tribological behaviour of Ti6Al4V and Inconel718 under dry and cryogenic conditions - Application to the context of machining with carbide tools. *Tribology International*, 66, pp.72–82. Available at: http://dx.doi.org/10.1016/j.triboint.2013.04.010.

Dargusch, M.S. et al., 2008. Subsurface deformation after dry machining of grade 2 titanium. *Advanced Engineering Materials*, 10(1-2), pp.85–88.

Edkinsa, K.D., Van Rensburga, N.J. & Laubscher, R.F., 2014. Evaluating the subsurface microstructure of machined Ti-6Al-4V. *Procedia CIRP*, 13, pp.270–275. Available at: http://dx.doi.org/10.1016/j.procir.2014.04.046.

El-Tayeb, N.S.M. et al., 2009. Modeling of cryogenic frictional behaviour of titanium alloys using Response Surface Methodology approach. *Materials and Design*, 30(10), pp.4023–4034. Available at: http://dx.doi.org/10.1016/j.matdes.2009.05.020.

Ezugwu, E.O., Bonney, J. & Yamane, Y., 2003. An overview of the machinability of aeroengine alloys. *Journal of Materials Processing Technology*, 134(2), pp.233–253.

Ezugwu, E.O. & Wang, Z.M., 1997. Titanium alloys and their machinability. *Journal of Materials Processing Technology*, 68(3), pp.262–274. Available at: http://www.sciencedirect.com/science/article/pii/S0924013696000301.

Hu, D. & Botten, R.R., 2002. Phase transformations in some TiAl-based alloys. *Intermetallics*, 10(7), pp.701–715.

Joshi, S., Tewari, A. & Joshi, S., 2014. Influence of Preheating on Chip Segmentation and Microstructure in Orthogonal Machining of Ti6Al4V. , 135(December 2013), pp.1–11.

Khanna, N. et al., 2012. Effect of heat treatment conditions on the machinability of Ti64 and Ti54M alloys. *Procedia CIRP*, 1(1), pp.477–482.

Kouadri, S. et al., 2013. Quantification of the chip segmentation in metal machining: Application to machining the aeronautical aluminium alloy AA2024-T351 with cemented carbide tools WC-Co. *International Journal of Machine Tools and Manufacture*, 64, pp.102–113.

Lee, I. et al., 2015. Tool life improvement in cryogenic cooled milling of the preheated Ti–6Al–4V. *The International Journal of Advanced Manufacturing Technology*, 79(1-4), pp.665–673.

Leyens, C. & Peters, M., 2006. *Titanium and Titanium Alloys*,

MacHai, C. & Biermann, D., 2011. Machining of β-titanium-alloy Ti-10V-2Fe-3Al under cryogenic conditions: Cooling with carbon dioxide snow. *Journal of Materials Processing Technology*, 211(6), pp.1175–1183. Available at: http://dx.doi.org/10.1016/j.jmatprotec.2011.01.022.

Matthew J. Donachie, J., 2000. *Titanium: A Technical Guide*,

Patil, S. et al., 2014. Modelling and simulation of effect of ultrasonic vibrations on machining of Ti6Al4V. *Ultrasonics*, 54(2), pp.694–705. Available at: http://dx.doi.org/10.1016/j.ultras.2013.09.010.

Popov, a. a. et al., 2014. Effect of quenching temperature on structure and properties of titanium alloy: Structure and phase composition. *The Physics of Metals and Metallography*, 115(5), pp.507–516.

Upadhyay, V., Jain, P.K. & Mehta, N.K., 2013. In-process prediction of surface roughness in turning of Ti-6Al-4V alloy using cutting parameters and vibration signals. *Measurement: Journal of the International Measurement Confederation*, 46(1), pp.154–160. Available at:

http://dx.doi.org/10.1016/j.measurement.2012.06.002.

Upadhyay, V., Jain, P.K. & Mehta, N.K., 2012. Machinability Studies in Hot Machining of Ti-6Al-4V Alloy. *Advanced Materials Research*, 622-623, pp.361–365.

Vrancken, B. et al., 2012. Heat treatment of Ti6Al4V produced by Selective Laser Melting: Microstructure and mechanical properties. *Journal of Alloys and Compounds*, 541, pp.177–185. Available at: http://dx.doi.org/10.1016/j.jallcom.2012.07.022.

Zhan, H. et al., 2014. The dynamic response of a β titanium alloy to high strain rates and elevated temperatures. *Materials Science and Engineering: A*, 607, pp.417–426. Available at: http://linkinghub.elsevier.com/retrieve/pii/S0921509314004730.